Hidden-charm strong decays of the Z_c states

Li-Ye Xiao,[1,*] Guang-Juan Wang,[2,3,†] and Shi-Lin Zhu[2,3,4,‡]

[1]*School of Mathematics and Physics, University of Science and Technology Beijing, Beijing 100083, China*
[2]*School of Physics and State Key Laboratory of Nuclear Physics and Technology, Peking University, Beijing 100871, China*
[3]*Center of High Energy Physics, Peking University, Beijing 100871, China*
[4]*Collaborative Innovation Center of Quantum Matter, Beijing 100871, China*

(Received 2 January 2020; accepted 16 February 2020; published 3 March 2020)

Inspired by BESIII's measurement of the decay $Z_c(3900)^{\pm} \to \rho^{\pm}\eta_c$, we calculate the branching fraction ratio between the $\rho\eta_c$ and $\pi J/\psi$ decay modes for the charged states $Z_c(3900)$, $Z_c(4020)$, and $Z_c(4430)$ using a quark interchange model. Our results show that (i) the ratio $R_{Z_c(3900)} = \frac{\mathcal{B}(Z_c(3900)^{\pm}\to\rho^{\pm}\eta_c)}{\mathcal{B}(Z_c(3900)^{\pm}\to\pi^{\pm}J/\psi)}$ is 1.3 and 1.6 in the molecular and tetraquark scenarios, respectively, which is roughly consistent with the experimental data $R^{\exp} = 2.2 \pm 0.9$, and (ii) the ratios $\frac{\Gamma[Z_c(3900)\to\rho\eta_c]}{\Gamma[Z_c(4020)\to\rho\eta_c]}$ and $\frac{\Gamma[Z_c(3900)\to\pi J/\psi]}{\Gamma[Z_c(4020)\to\pi J/\psi]}$ are about 12.5 and 24.2, respectively, in the molecular scenario. In contrast, these ratios are about 1.2 in the tetraquark scenario. The nonobservation of the $Z_c(4020)$ signal in the $\pi J/\psi$ decay mode strongly indicates that $Z_c(3900)$ and $Z_c(4020)$ are moleculelike signals which arise from the $D^{(*)}\bar{D}^{(*)}$ hadronic interactions.

DOI: 10.1103/PhysRevD.101.054001

I. INTRODUCTION

Since 2003, when the Belle Collaboration observed the first charmoniumlike state [1], $X(3872)$, an explosion in the observation of new hadronic states began. Dozens of charmoniumlike states (or XYZ states) [2] have been reported by major experimental collaborations such as BESIII, LHCb, Belle, *BABAR*, CDF, and so on; see Refs. [3–8] for reviews. The properties of the charged Z_c states cannot be explained by the naive quark model and make them manifestly exotic. It seems that we have a new zoo of exotic hadrons. How to understand their internal structures remains a great challenge.

The charged charmoniumlike state $Z_c(4430)$ [9–14] was first observed Z_c in 2007, which has triggered extensive theoretical speculations such as the molecular state [15], the first radial tetraquark excitation [16–18], threshold cusp effects [19], and triangle singularities [20]. In 2003, $Z_c(3900)$ [21–23] and $Z_c(4020)$ [24] were observed. There are also many model-dependent interpretations of their inner structures, such as the $D^{(*)}\bar{D}^{(*)}$ molecular states [25–31], the S-wave tetraquark states [16,32–37], and the kinematical effects [38–42].

Recently, the BESIII Collaboration reported the first evidence of the decay $Z_c(3900)^{\pm} \to \rho^{\pm}\eta_c$ with a statistical significance of 3.9σ in the $\pi^+\pi^-\pi^0\eta_c$ final state [43]. The BESIII Collaboration also gave the ratio between the partial widths of the $\rho^{\pm}\eta_c$ and $\pi^{\pm}J/\psi$ decay modes at $\sqrt{s} = 4.226$ GeV [43]:

$$R^{\exp}_{Z_c(3900)} = \frac{\mathcal{B}(Z_c(3900)^{\pm} \to \rho^{\pm}\eta_c)}{\mathcal{B}(Z_c(3900)^{\pm} \to \pi^{\pm}J/\psi)} = 2.2 \pm 0.9. \quad (1)$$

Before BESIII's measurement [43], the relative decay rate was predicted in either the molecular or tetraquark scenarios within the framework of a covariant quark model [44], the phenomenological Lagrangian field theory [45], the nonrelativistic effective field theory [46], the light front model [47], QCD sum rules [48–50], etc., Later, Chen [51] studied the decay properties of the $Z_c(3900)$ as a compact tetraquark state and a hadronic molecular state through the Fierz rearrangement of the Dirac and color indices. We collect the theoretical predictions, which differ greatly, in Table I.

In this work, we calculate the ratio between the $\rho\eta_c$ and $\pi J/\psi$ decay modes for the charged states $Z_c(3900)$, $Z_c(4020)$, and $Z_c(4430)$ in two different scenarios. In scenario I, we take the $Z_c(3900)$, $Z_c(4020)$, and $Z_c(4430)$ as the $D\bar{D}^*$, $D^*\bar{D}^*$, and $D(2S)\bar{D}^*$ molecular states with spin parity $J^P = 1^+$, respectively. In scenario II, we treat the $Z_c(3900)$, $Z_c(4020)$, and $Z_c(4430)$ as the tetraquark states.

*lyxiao@ustb.edu.cn
†wgj@pku.edu.cn
‡zhusl@pku.edu.cn

TABLE I. The theoretical predictions of $R_{Z_c(3900)}$ in various models.

Experiment	Molecular	Tetraquark
2.2 ± 0.9 [43]	$0.046^{+0.025}_{-0.017}$ [46]	230^{+330}_{-140} [46]
	$1.78^{+0.41}_{-0.37}$ [44]	$0.27^{+0.40}_{-0.17}$ [46]
	0.12 [47]	$1.86^{+0.41}_{-0.35}$ [44]
	0.007 [45]	$1.28^{+0.37}_{-0.30}$ [44]
	0.059 [51]	2.2 [51]
		1.08 ± 0.88 [49]
		0.95 ± 0.40 [48]
		0.66 [36]
		0.57 ± 0.17 [50]

Our results show that in the molecular and tetraquark scenarios, the ratios for $Z_c(3900)$ are $R^{\rm th}_{Z_c(3900)} \simeq 1.3$ and $R^{\rm th}_{Z_c(3900)} \simeq 1.6$, respectively, which are both in the range of experimental result, $R^{\rm exp} = 2.2 \pm 0.9$. For $Z_c(4020)$, the ratio is about $R^{\rm th}_{Z_c(4020)} \sim 2$ in both two scenarios. As for $Z_c(4430)$, we find that the ratio in the molecular scenario ($R^{\rm th}_{Z_c(4430)} \simeq 1.4$) is slightly smaller than that in the tetraquark scenario [$R^{\rm th}_{Z_c(4430)} \simeq (1.7$–$1.4)$].

We notice that the ratios $\frac{\Gamma[Z_c(3900)\to\rho\eta_c]}{\Gamma[Z_c(4020)\to\rho\eta_c]}$ and $\frac{\Gamma[Z_c(3900)\to\pi J/\psi]}{\Gamma[Z_c(4020)\to\pi J/\psi]}$ are about 12.5 and 24.2, respectively, in the molecular scenario. However, both ratios are about 1.2 in the tetraquark scenario. In other words, these ratios are very sensitive to the underlying dynamics of $Z_c(3900)$ and $Z_c(4020)$, which may be helpful for pinning down their inner structures.

This paper is organized as follows. In Sec. II, we give an introduction of the quark-exchange model and calculate the transition amplitudes in the molecular and tetraquark scenarios. Then we discuss and compare our results in the two scenarios in Sec. III. We give a short summary in Sec. IV.

II. MODEL INTRODUCTION

A. Decay width

For a four-quark state (F for short) decaying into two particles labeled C and D, the decay width in the rest frame of the initial particle has the form

$$d\Gamma = \frac{|\vec{p}_c|}{32\pi^2 M^2}|\mathcal{M}(F \to C + D)|^2 d\Omega. \tag{2}$$

Here, M represents the mass of the initial four-quark state F; $\vec{p}_c$ denotes the three-momentum of the meson C in the final state; and $\mathcal{M}(F \to C + D)$ is the transition amplitude of the two-body decay $F \to C + D$, which is related to the T-matrix via

$$\mathcal{M}(F \to C + D) = -(2\pi)^{3/2}\sqrt{2M}\sqrt{2E_C}\sqrt{2E_D}T, \tag{3}$$

where E_C and E_D denote the energy of the final mesons C and D, respectively. The T-matrix reads

$$\begin{aligned} T &= \langle \psi_{CD}(\vec{p}_c)|V_{\rm eff}(\vec{k}, \vec{p}_c)|\psi_F(\vec{k})\rangle \\ &= \langle \psi_{CD}(\vec{p}_c)|V_{\rm eff}(\vec{k}, \vec{p}_c)|\psi_{AB}(\vec{k})\rangle. \end{aligned} \tag{4}$$

Here, $\psi_{CD}(\vec{p}_c)$ represents the relative spacial wave function between the final mesons C and D; $\psi_{AB}(\vec{k})$ is the normalized relative spacial wave function between the constituent clusters A and B. In the molecular scenario, the constituents represent mesons, while in the tetraquark scenario the constituents represent the diquark $[cq]$ and antidiquark $[\bar{c}\,\bar{q}]$. $V_{\rm eff}(\vec{k}, \vec{p}_c)$ denotes the effective potential, which is, in the general case, a function of the initial and final relative momenta $\vec{k}$ and $\vec{p}_c$.

The four-quark state may be a superposition of terms with different orbital angular momenta.[1] Thus, the relative spacial wave function in the momentum space has the form

$$\psi_{AB}(\vec{k}) = \sum_l R_l(k) Y_{lm}(\vec{k}). \tag{5}$$

Then Eq. (4) can be written as

$$\begin{aligned} T &= \frac{1}{(2\pi)^3}\int d\vec{k}\int d\vec{p}\,\delta(\vec{p} - \vec{p}_c)V_{\rm eff}(\vec{k}, \vec{p})\sum_l R_l(k)Y_{lm}(\vec{k}) \\ &= \frac{1}{(2\pi)^2}\sum_l M_{ll}Y_{lm}(\vec{p}_c), \end{aligned} \tag{6}$$

where

$$M_{ll} = \int_{-1}^{1} P_l(\mu)d\mu \int dk V_{\rm eff}(\vec{k}, \vec{p}_c, \mu)R_l(k)k^2. \tag{7}$$

In this equation, $P_l(\mu)$ is the Legendre function and μ represents the cosine of the angle between the momenta $\vec{k}$ and $\vec{p}_c$.

Finally, with the relativistic phase space, the decay width of the two-body decay process reads

$$\Gamma_{\pi J/\psi} = \frac{E_C E_D|\vec{p}_c|}{(2\pi)^3 M}|M_{ll}|^2. \tag{8}$$

For the $\rho\eta_c$ decay mode, we further consider the decay width of the ρ meson and get

$$\Gamma_{\rho\eta_c} = \frac{1}{N}\int ds \frac{E_C E_D|\vec{p}_c|}{(2\pi)^3 M}|M_{ll}|^2 \frac{1}{\pi}\frac{m_\rho\Gamma_\rho}{(s - m_\rho^2)^2 + (m_\rho\Gamma_\rho)^2}, \tag{9}$$

with

[1]We assume that the orbital excitation is between the diquark and the antidiquark.

$$N = \int ds \frac{1}{\pi} \frac{m_\rho \Gamma_\rho}{(s - m_\rho^2)^2 + (m_\rho \Gamma_\rho)^2}. \quad (10)$$

Here, m_ρ and Γ_ρ stand for the mass and total decay width of the ρ meson, respectively. s denotes the square of the ρ meson energy.

B. Effective potential

1. The molecular scenario

The J^P quantum number of the $Z_c(3900)$, $Z_c(4020)$, and $Z_c(4430)$ are 1^+. In the molecular scenario, we treat them as the loosely bound S-wave $D\bar{D}^*$, $D^*\bar{D}^*$, and $D(2S)\bar{D}^*$ molecular states, respectively, according to their mass spectra. At Born order, the effective potential $V_{\rm eff}(\vec{k}, \vec{p}_c, \mu)$ is related to the reacting amplitude of the meson-meson scattering process,

$$A(12) + B(34) \to C(13) + D(24), \quad (11)$$

where 1(3) and 2(4) denote the $c(\bar{c})$ quark and $\bar{q}(q)$ quark, respectively. In the quark interchange model [52–56], the hadron-hadron scattering process is approximated by the interaction between the inner quarks. Thus, the scattering Hamiltonian of the processes $D^{(*)}/D(2S) + \bar{D}^* \to \eta_c(J/\psi) + \rho(\pi)$ is estimated by the sum of the interactions between the inner quarks as illustrated in Fig. 1. Moreover, the short-range interactions are dominant in the scattering processes of two open-charmed mesons into a ground charmonium state plus a light-flavor meson. Thus, the scattering potential can be approximated by the one-gluon-exchange potential V_{ij} at quark level[2]

$$V_{ij} = \frac{\lambda_i}{2}\frac{\lambda_j}{2}\left\{\frac{4\pi\alpha_s}{q^2} + \frac{6\pi b}{q^4} - \frac{8\pi\alpha_s}{3m_i m_j}\mathbf{s}_i \cdot \mathbf{s}_j e^{-\frac{q^2}{4\sigma^2}}\right\}, \quad (12)$$

where $\lambda_i(\lambda_i^T)$ represents the quark (antiquark) generator; q is the transferred momentum, b denotes the string tension; σ is the range parameter in the hyperfine spin-spin interaction; $m_i(m_j)$ and $\mathbf{s}_i(\mathbf{s}_j)$ correspond to the interacting constituent quark mass and spin operator, respectively; and α_s is the running coupling constant,

$$\alpha_s(Q^2) = \frac{12\pi}{(33 - 2n_f)\ln(A + Q^2/B^2)}. \quad (13)$$

In this equation, Q^2 is the square of the invariant masses of the interacting quarks. The parameters in Eqs. (12) and (13) are fitted by the mass spectra of the observed mesons [57], and their values are listed in Table II.

[2]The interactions in Eq. (12) are the Fourier transformation of the potential in Ref. [57]. In the following. we perform our calculations in the momentum space for the purpose of simplification. The constant potential in the spatial space does not contribute due to the cancelation of the form factors, and we just omitted the term in Eq. (12).

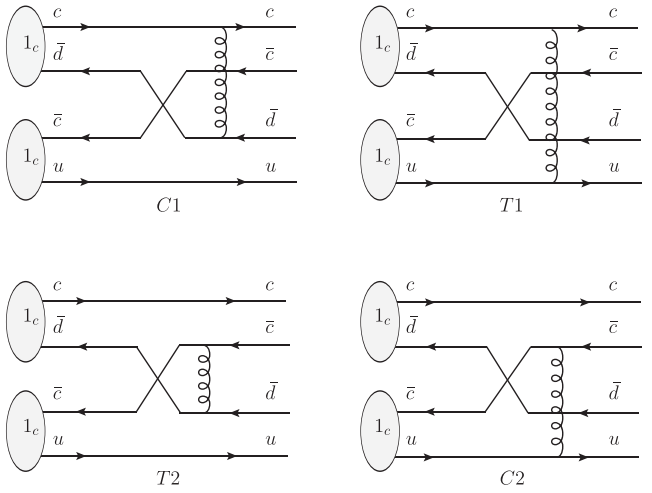

FIG. 1. Diagrams for the scattering process $AB \to CD$ in the molecular scenario.

In the quark model, the color-spin-flavor-space wave function for a meson is

$$\Psi = \omega_c \phi_f \chi_s \psi(\vec{p}), \quad (14)$$

where ω_c, ϕ_f, χ_s, and $\psi(\vec{p})$ represent the wave functions in the color, flavor, spin, and momentum space, respectively. Here, the wave functions of the mesons are determined by fitting the mass spectra in the Godfrey-Isgur model [58].

According to the decomposition of the meson wave functions, the effective potential can be given as the product of the factors,

$$V_{\rm eff}(\vec{k}, \vec{p}_c, \mu) = I_{\rm color} I_{\rm flavor} I_{\text{spin-space}}. \quad (15)$$

Here, I with the subscripts color, flavor and spin-space represent the overlaps of the initial and final wave functions in the corresponding space. The color factor $I_{\rm color}$ reads

$$I_{\rm color} = \langle \omega_c^C(13)\omega_c^D(24)|\frac{\lambda_i}{2}\cdot\frac{\lambda_j}{2}|\omega_c^A(12)\omega_c^B(34)\rangle. \quad (16)$$

Its value in different diagrams in Fig. 1 is listed in Table III. For the flavor factor $I_{\rm flavor}$, its value is simply unity for all diagrams considered in this paper.

TABLE II. The parameters [57] used in the quark model.

Parameter	b	0.18 GeV^2
	σ	0.897 GeV
	A	10
	B	0.31 GeV
Constituent quark mass	m_q	0.334 GeV
	m_c	1.776 GeV

TABLE III. The color factor I_{color} within the molecular scenario.

	$12(C1)$	$14(T1)$	$32(T2)$	$34(C2)$
I_{color}	$-\frac{4}{9}$	$\frac{4}{9}$	$\frac{4}{9}$	$-\frac{4}{9}$

For the S-wave decay process, the spin and space factors can be decoupled. The spin factor I_{spin} reads

$$I_{\text{spin}} = \langle [\chi_s^C(13)\chi_s^D(24)]_{S'} | \hat{\mathcal{O}}_s | [\chi_s^A(12)\chi_s^B(34)]_S \rangle, \tag{17}$$

where S (S') stands for the total spin of the initial (final) system. The spin operator $\hat{\mathcal{O}}_s$ equals unity for the Coulomb and linear interactions, and equals $\mathbf{s_i} \cdot \mathbf{s_j}$ for the spin-spin interaction. We collect the values of color-spin factors $I_{\text{color}} \cdot I_{\text{spin}}$ in Table IV.

As for the spatial factor I_{space}, its expression reads

$$I_{\text{space}}^{C1} = \iint d\vec{q} d\vec{p}_3 \psi_A(-\vec{q} - \vec{p}_3 + \vec{p}_c - f_1\vec{k}) \psi_B(\vec{p}_3 + f_2\vec{k}) \times \hat{\mathcal{O}}_q \psi_C^*(-\vec{p}_3 + f_3\vec{p}_c) \psi_D^*(\vec{p}_3 - f_4\vec{p}_c + \vec{k}), \tag{18}$$

$$I_{\text{space}}^{T1} = \iint d\vec{q} d\vec{p}_3 \psi_A(-\vec{q} - \vec{p}_3 + \vec{p}_c - f_1\vec{k}) \psi_B(\vec{p}_3 + f_2\vec{k}) \times \hat{\mathcal{O}}_q \psi_C^*(-\vec{p}_3 + f_3\vec{p}_c) \psi_D^*(\vec{q} + \vec{p}_3 - f_4\vec{p}_c + \vec{k}), \tag{19}$$

$$I_{\text{space}}^{T2} = \iint d\vec{q} d\vec{p}_3 \psi_A(-\vec{p}_3 + \vec{p}_c - f_1\vec{k}) \psi_B(\vec{p}_3 + f_2\vec{k}) \times \hat{\mathcal{O}}_q \psi_C^*(\vec{q} - \vec{p}_3 + f_3\vec{p}_c) \psi_D^*(\vec{p}_3 - f_4\vec{p}_c + \vec{k}), \tag{20}$$

$$I_{\text{space}}^{C2} = \iint d\vec{q} d\vec{p}_3 \psi_A(-\vec{q} - \vec{p}_3 + \vec{p}_c - f_1\vec{k}) \psi_B(\vec{p}_3 + f_2\vec{k}) \times \hat{\mathcal{O}}_q \psi_C^*(-\vec{q} - \vec{p}_3 + f_3\vec{p}_c) \psi_D^*(\vec{q} + \vec{p}_3 - f_4\vec{p}_c + \vec{k}). \tag{21}$$

In the equations, the spatial operator $\hat{\mathcal{O}}_q$ corresponds to $1/q^2$, $1/q^4$, and $e^{-q^2/(4\sigma^2)}$ for the Coulomb, linear, and spin-spin interactions, respectively. $\vec{p}_3$ denotes the momentum of the third quark. $f_i (i = 1, 2, 3, 4)$ is a constituent quark mass-dependent function and is expressed as

$$f_1 = \frac{m_1}{m_1 + m_2}, \qquad f_2 = \frac{m_3}{m_3 + m_4}, \tag{22}$$

$$f_3 = \frac{m_3}{m_1 + m_3}, \qquad f_4 = \frac{m_4}{m_2 + m_4}. \tag{23}$$

Here, $m_i (i = 1, 2, 3, 4)$ represents the mass of the ith quark.

Finally, with the obtained effective potential $V_{\text{eff}}(\vec{k}, \vec{p}_c, \mu)$, we can calculate the decay widths by Eqs. (8) and (9) in cases that we know the relative spacial wave function $\psi_{AB}(\vec{k})$ between mesons A and B. In this work, we adopt an S-wave harmonic oscillator function to estimate the S-wave component of the relative spacial wave function in Eq. (5), which reads

$$R_{00}(\vec{k}) = \frac{2e^{-\frac{k^2}{2\alpha^2}}}{\pi^{1/4}\alpha^{3/2}}. \tag{24}$$

The value of the harmonic oscillator strength α is related to the root mean square radius r_{mean} of the molecular state by $\frac{\sqrt{3}}{\sqrt{2}\alpha} = r_{\text{mean}}$. Here, we take the r_{mean} in the range of (1.0–3.0) fm, and the corresponding value of α is collected in Table V.

TABLE IV. The values of color-spin factors for the diagrams [$C1$, $T1$, $T2$, $C2$] within the molecular scenario. Here, $D^{(*)}/D(2S)\bar{D}^*$ is the shorthand for $D^{(*)}/D(2S)\bar{D}^* + \text{c.c.}$

Initial state	Final state	Coulomb and linear	Hyperfine
$D\bar{D}^*$	$\eta_c\rho$	$\frac{2}{9}[-1,1,1,-1]$	$\frac{1}{18}[3,-1,3,-1]$
	$J/\psi\pi$	$-\frac{2}{9}[-1,1,1,-1]$	$\frac{1}{18}[-3,-3,1,1]$
$D^*\bar{D}^*$	$\eta_c\rho$	$\frac{2\sqrt{2}}{9}[-1,1,1,-1]$	$-\frac{\sqrt{2}}{18}[1,1,1,1]$
	$J/\psi\pi$	$\frac{2\sqrt{2}}{9}[-1,1,1,-1]$	$-\frac{\sqrt{2}}{18}[1,1,1,1]$
$D(2S)\bar{D}^*$	$\eta_c\rho$	$\frac{2}{9}[-1,1,1,-1]$	$\frac{1}{18}[3,-1,3,-1]$
	$J/\psi\pi$	$-\frac{2}{9}[-1,1,1,-1]$	$\frac{1}{18}[-3,-3,1,1]$

2. The tetraquark scenario

For comparison, we further study the decays of the $Z_c(3900)$, $Z_c(4020)$, and $Z_c(4430)$ as tetraquark states $c\bar{c}q\bar{q}$ [18],

$$\begin{aligned} Z_c(3900)&: \frac{1}{\sqrt{2}}\{[[cu]_{\bar{3}_c}^{s=0}[\bar{c}\,\bar{d}]_{3_c}^{s=1}]_{1_c}^{s=1} + [[cu]_{\bar{3}_c}^{s=1}[\bar{c}\,\bar{d}]_{3_c}^{s=0}]_{1_c}^{s=1}\}, \\ Z_c(4020)&: [[cu]_{\bar{3}_c}^{s=1}[\bar{c}\,\bar{d}]_{3_c}^{s=1}]_{1_c}^{s=1}, \\ Z_c(4430)&: \frac{1}{\sqrt{2}}\{[[cu]_{\bar{3}_c}^{s=0}[\bar{c}\,\bar{d}]_{3_c}^{s=1}]_{1_c}^{s=1} + [[cu]_{\bar{3}_c}^{s=1}[\bar{c}\,\bar{d}]_{3_c}^{s=0}]_{1_c}^{s=1}\}, \end{aligned} \tag{25}$$

where $Z_c(4430)$ is interpreted as the first radial excitation of the $Z_c(3900)$.

Similar to the molecular case, the $V_{\text{eff}}(\vec{k}, \vec{p}_c, \mu)$ can be approximated by the interaction between the inner quarks, as shown in Fig. 2.

TABLE V. The corresponding values of the harmonic oscillator strength α between the constituent mesons A and B in the molecular scenario.

$\sqrt{\langle r_{\text{mean}}\rangle^2}$ (fm)	1.0	1.2	1.5	1.7	2.0	2.4	3.0
α (GeV)	0.21	0.18	0.16	0.14	0.12	0.10	0.08

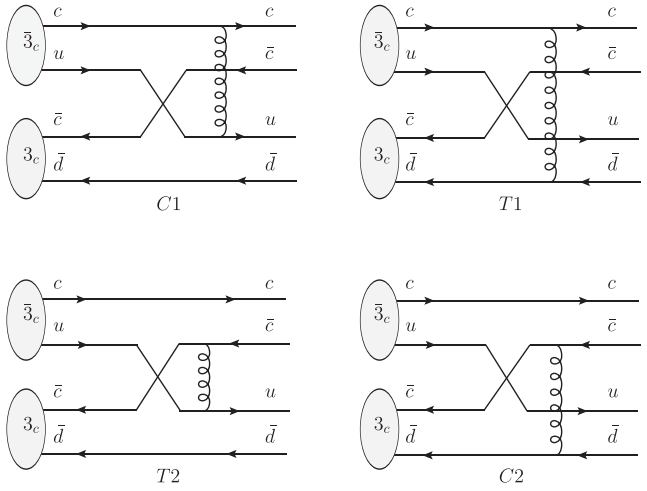

FIG. 2. Diagrams for the scattering process $AB \to CD$ in the tetraquark scenario.

The calculation of the $V_{\rm eff}(\vec{k}, \vec{p}_c, \mu)$ in the tetraquark scenario is similar to that in the molecular scenario. We can obtain the effective potential $V_{\rm eff}(\vec{k}, \vec{p}_c, \mu)$ with Eq. (15) as well. The flavor factor $I_{\rm flavor}$ and spin factor $I_{\rm spin}$ are the same as those in the molecular scenario. For the color factor $I_{\rm color}$, there is a difference between the two scenarios. In the molecular scenario, the initial four-quark state is composed of two mesons, of which the color configurations are 1_c-1_c. However, in the tetraquark scenario, the initial four-quark state is composed of diquark $[cq]$ and antidiquark $[\bar{c}\,\bar{q}]$, of which the color configurations are 3_c-$\bar{3}_c$. The difference in color configurations may result in quite different decay properties. The values of color-spin factors are collected in Table VI.

To calculate the space factor $I_{\rm space}$, we need the wave function of the initial tetraquark state,

$$\begin{aligned}\Psi(\vec{k}_r, \vec{k}_R, \vec{k}_X) &= \psi_A(\vec{k}_r, \alpha_r)\psi_B(\vec{k}_R, \alpha_R)\psi_{AB}(\vec{k}_X, \alpha_X) \\ &\times [\chi_{s_a}(cu)\chi_{s_b}(\bar{c}\,\bar{d})]^{S_z}_S[\omega_{\bar{3}_c}(cu)\omega_{3_c}(\bar{c}\,\bar{d})]_{1_c} \\ &\times [\phi_{I_a}(cu)\phi_{I_b}(\bar{c}\,\bar{d})]^{I_z}_I, \end{aligned} \tag{26}$$

where $\vec{k}_{r/R}$ denotes the momentum between the $c(\bar{c})$ and $u(\bar{d})$ quarks in the diquark (antidiquark), and where $\vec{k}_X$ is the one between the diquark $[cu]$ and antidiquark $[\bar{c}\,\bar{d}]$. The α's with the subscripts represent the oscillating parameter along the corresponding Jacobi coordinates.

For $Z_c(3900)$ and $Z_c(4020)$, the spatial wave function ψ is estimated by the S-wave harmonic oscillating wave function,

$$\psi(\vec{k}, \alpha) = \frac{1}{\pi^{3/4}\alpha^{3/2}} e^{-\frac{k^2}{2\alpha^2}}. \tag{27}$$

The α values are taken from Ref. [37], in which Deng *et al.* presented a systematic study of the tetraquark states $[cu][\bar{c}\,\bar{d}]$ with the color flux-tube model and predicted that the charged charmoniumlike states $Z_c(3900)$ could be identified as the tetraquark state $[cu][\bar{c}\,\bar{d}]$ with the quantum numbers 1^3S_1 and $J^P = 1^+$, as listed in Table VII. For $Z_c(4020)$, we give its wave function via imitating the wave function of $Z_c(3900)$, listed in Table VII as well. It should be remarked that the spin of the diquark $[cu]$ and antidiquark $[\bar{c}\,\bar{d}]$ both equal unity for $Z_c(4020)$.

As for $Z_c(4430)$, the spatial wave function of the diquark $[cu]$ is replaced by that of D, and the spatial wave function of antidiquark $[\bar{c}\,\bar{d}]$ is replaced by that of D^*. The relative spatial wave function between the diquark $[cu]$ and antidiquark $[\bar{c}\,\bar{d}]$ is estimated by a $2S$-wave harmonic oscillating space-wave function

$$R_{10}(k_X) = \frac{\sqrt{6}e^{-\frac{k_X^2}{2\alpha_X^2}}}{\pi^{1/4}\alpha_X^{3/2}}\left(1 - \frac{2k_X^2}{3\alpha_X^2}\right). \tag{28}$$

The value of the harmonic oscillator strength α_X is related to the root mean square radius r_X of the tetraquark state by $\frac{\sqrt{7}}{\sqrt{2}\alpha_X} = r_X$. We vary r_X in the range (0.5–2.0) fm, and the corresponding value of α_X is listed in Table VIII.

TABLE VI. The values of the color-spin factors for the diagrams [$C1$, $T1$, $T2$, $C2$] within the tetraquark scenario.

Initial state	Final state	Coulomb and linear	Hyperfine
$Z_c(3900)[[cu]^{S=0}_{\bar{3}_c}[\bar{c}\,\bar{d}]^{S=1}_{3_c}]^{S=1}_{1_c}$	$\eta_c\rho$	$\frac{1}{3\sqrt{3}}[-1,1,1,-1]$	$[\frac{1}{4\sqrt{3}},-\frac{1}{12\sqrt{3}},\frac{1}{4\sqrt{3}},-\frac{1}{12\sqrt{3}}]$
	$J/\psi\pi$	$-\frac{1}{3\sqrt{3}}[-1,1,1,-1]$	$[-\frac{1}{4\sqrt{3}},-\frac{1}{4\sqrt{3}},\frac{1}{12\sqrt{3}},\frac{1}{12\sqrt{3}}]$
$Z_c(4020)[[cu]^{S=1}_{\bar{3}_c}[\bar{c}\,\bar{d}]^{S=1}_{3_c}]^{S=1}_{1_c}$	$\eta_c\rho$	$\frac{2}{3\sqrt{6}}[-1,1,1,-1]$	$[-\frac{1}{6\sqrt{6}},-\frac{1}{6\sqrt{6}},-\frac{1}{6\sqrt{6}},-\frac{1}{6\sqrt{6}}]$
	$J/\psi\pi$	$\frac{2}{3\sqrt{6}}[-1,1,1,-1]$	$[-\frac{1}{6\sqrt{6}},-\frac{1}{6\sqrt{6}},-\frac{1}{6\sqrt{6}},-\frac{1}{6\sqrt{6}}]$
$Z_c(4430)[[cu]^{S=0}_{\bar{3}_c}[\bar{c}\,\bar{d}]^{S=1}_{3_c}]^{S=1}_{1_c}$	$\eta_c\rho$	$\frac{1}{3\sqrt{3}}[-1,1,1,-1]$	$[\frac{1}{4\sqrt{3}},-\frac{1}{12\sqrt{3}},\frac{1}{4\sqrt{3}},-\frac{1}{12\sqrt{3}}]$
	$J/\psi\pi$	$-\frac{1}{3\sqrt{3}}[-1,1,1,-1]$	$[-\frac{1}{4\sqrt{3}},-\frac{1}{4\sqrt{3}},\frac{1}{12\sqrt{3}},\frac{1}{12\sqrt{3}}]$

TABLE VII. The rms of the tetraquark states $[cu][\bar{c}\,\bar{d}]$. $\sqrt{\langle r\rangle^2}(\sqrt{\langle R\rangle^2})$ denotes the distance between the $c(\bar{c})$ and $u(\bar{u})$ quarks, and $\sqrt{\langle X\rangle^2}$ is the distance between the diquark $[cu]$ and antidiquark $[\bar{c}\,\bar{u}]$. The unit of rms is fm.

States	Tetraquark	$\sqrt{\langle r\rangle^2}$	$\sqrt{\langle R\rangle^2}$	$\sqrt{\langle X\rangle^2}$
$Z_c(3900)$ [37]	$[[cu]^{S=0}_{\bar{3}_c}[\bar{c}\,\bar{u}]^{S=1}_{3_c}]^{S=1}_{1_c}$	0.90	0.90	0.48
$Z_c(4020)$	$[[cu]^{S=1}_{\bar{3}_c}[\bar{c}\,\bar{u}]^{S=1}_{3_c}]^{S=1}_{1_c}$	0.90	0.90	0.48

TABLE VIII. The corresponding values of the harmonic oscillator strength α_X between the diquark $[cu]$ and the antidiquark $[\bar{c}\,\bar{d}]$ for $Z_c(4430)$ as a tetraquark state.

$\sqrt{\langle r_X\rangle^2}$ (fm)	0.5	0.8	1.0	1.5	2.0
α_X (GeV)	0.74	0.46	0.37	0.25	0.18

III. RESULTS

Inspired by the recent measurement of the decay $Z_c(3900)^{\pm} \to \rho^{\pm}\eta_c$ by the BESIII Collaboration, we calculate the ratios between the $\rho\eta_c$ and $\pi J/\psi$ decay modes for the charged states $Z_c(3900)$, $Z_c(4020)$, and $Z_c(4430)$ in the molecular and tetraquark scenarios. Our results and theoretical predictions are presented as follows.

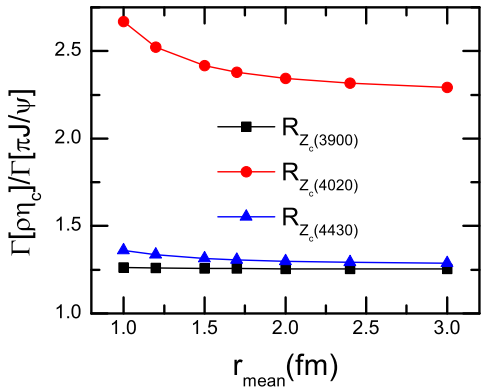

FIG. 3. The variation of the partial decay width ratios between the $\eta_c\rho$ and $J/\psi\pi$ channels for the $Z_c(3900)$, $Z_c(4020)$, and $Z_c(4430)$ as the $D\bar{D}^*$, $D^*\bar{D}^*$, and $D(2S)\bar{D}^*$ molecular states, respectively. Their masses are fixed, respectively, on physical masses—namely, 3886.6, 4024.1, and 4478 MeV.

A. The molecular scenario

The mass of $Z_c(3900)$ ($M = 3886.6 \pm 2.4$ MeV) is slightly higher than the mass threshold of the $D\bar{D}^*(\sim 3872$ MeV). In the molecular scenario, we take $Z_c(3900)$ as a $D\bar{D}^*$ resonance molecular state and calculate its branching fraction ratio between the $\rho\eta_c$ and $\pi J/\psi$ decay modes. Considering the uncertainty of the effective size for the molecular state, we plot the ratio as a function of the root mean square radius $r_{\rm mean}$ in Fig. 3. The ratio is

$$R^{\rm th}_{Z_c(3900)} \sim 1.3, \tag{29}$$

which is roughly in accord with the experimental result $R^{\rm exp}_{Z_c(3900)} = 2.2 \pm 0.9$ [43] within errors. Meanwhile, the ratio is insensitive to $r_{\rm mean}$ in the range (1.0–3.0) fm we considered in this work.

With the estimated relative spacial wave function illustrated in Eq. (24), we further obtain the partial widths of the $\eta_c\rho$ and $J/\psi\pi$ decay modes and show them in Fig. 4. It is obvious that the partial widths are sensitive to $r_{\rm mean}$ and vary from 1 to $\mathcal{O}(10^{-2})$ MeV. With $r_{\rm mean}$ increasing, the partial decay widths become smaller, or even close to zero. This can be easily understood since the larger $r_{\rm mean}$ means the freer mesons A and B. It is more difficult to interact with each other, and the effective potential tends to vanish.

Moreover, for an S-wave molecule composed of two mesons A and B, its size may be estimated by [6,59,60]

$$r_{\rm mean} \sim 1/\sqrt{2\mu|m_A + m_B - M|}, \tag{30}$$

with the reduced mass $\mu = \frac{m_A m_B}{m_A + m_B}$. Then the typical size of $Z_c(3900)$ is estimated to be $r_{\rm mean} \simeq 1.14$ fm. Hence we obtain

$$\begin{aligned}\Gamma[Z_c(3900) \to \eta_c\rho] &\sim 2.76 \text{ MeV},\\ \Gamma[Z_c(3900) \to J/\psi\pi] &\sim 2.18 \text{ MeV},\end{aligned} \tag{31}$$

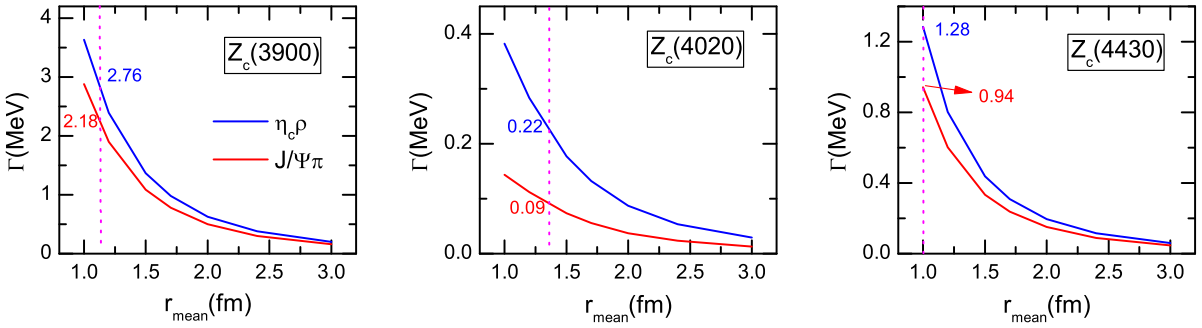

FIG. 4. The partial widths of the $\eta_c\rho$ and $J/\psi\pi$ decay modes for $Z_c(3900)$, $Z_c(4020)$, and $Z_c(4430)$ as the $D\bar{D}^*$, $D^*\bar{D}^*$, and $D(2S)\bar{D}^*$ molecular states, respectively. Their masses are fixed, respectively, on the physical masses—namely, 3886.6, 4024.1, and 4478 MeV.

TABLE IX. The partial decay widths (MeV) for the $Z_c(3900)$, $Z_c(4020)$, and $Z_c(4430)$ as the molecular states with typical size $r_{\rm mean}$ (fm). $R^{\rm th}$ and $R^{\rm exp}$ are theoretical and experimental ratios, respectively.

State	$r_{\rm mean}$	$\Gamma[\eta_c\rho]$	$\Gamma[J/\psi\pi]$	$R^{\rm th}$	$R^{\rm exp}$
$Z_c(3900)$	1.14	2.76	2.18	1.3	2.2 ± 0.9
$Z_c(4020)$	1.37	0.22	0.09	2.4	$\cdots$
$Z_c(4430)$	1.00	1.28	0.94	1.4	$\cdots$

for $Z_c(3900)$ with a mass of $M = 3886.6$ MeV (see Table IX).

We take $Z_c(4020)$ as the S-wave $D^*\bar{D}^*$ resonance molecular state since its mass ($M = 4024.1$ MeV) is slightly about 10 MeV higher than the mass threshold of the $D^*\bar{D}^*$. With the molecular size varying in the range $r_{\rm mean} = (1.0$–$3.0)$ fm, we calculate its partial decay width ratio between the $\eta_c\rho$ and $J/\psi\pi$ modes and obtain

$$R^{\rm th}_{Z_c(4020)} \sim (2.7 \sim 2.3), \tag{32}$$

with the mass being $M = 4024.1$ MeV (see Fig. 3). This value is almost independent of the $r_{\rm mean}$ we considered in this work.

We also plot the partial decay widths of the $\eta_c\rho$ and $J/\psi\pi$ modes versus the molecular size $r_{\rm mean}$ in Fig. 4. In the figure, we find that the partial widths are about $\mathcal{O}(10^{-1}$–$10^{-2})$ MeV, and strongly dependent on $r_{\rm mean}$. Fixing $r_{\rm mean} \simeq 1.37$ fm estimated by Eq. (30), we obtain

$$\begin{aligned}\Gamma[Z_c(4020) \to \eta_c\rho] &\sim 0.22 \text{ MeV},\\ \Gamma[Z_c(4020) \to J/\psi\pi] &\sim 0.09 \text{ MeV}.\end{aligned} \tag{33}$$

The predicted branching ratios are

$$\begin{aligned}\mathcal{B}[Z_c(4020) \to \eta_c\rho] &\sim 1.7\%,\\ \mathcal{B}[Z_c(4020) \to J/\psi\pi] &\sim 0.7\%.\end{aligned} \tag{34}$$

which are quite small.

The partial widths of the $\eta_c\rho$ and $J/\psi\pi$ decay modes for $Z_c(4020)$ are smaller than those for $Z_c(3900)$,

$$\frac{\Gamma[Z_c(3900) \to \eta_c\rho]}{\Gamma[Z_c(4020) \to \eta_c\rho]} = 12.5, \tag{35}$$

$$\frac{\Gamma[Z_c(3900) \to J/\psi\pi]}{\Gamma[Z_c(4020) \to J/\psi\pi]} = 24.2. \tag{36}$$

This indicates that the couplings of $D\bar{D}^*$ to the $\eta_c\rho$ and $J/\psi\pi$ channels are stronger than those of $D^*\bar{D}^*$. The main difference between $D\bar{D}^*$ and $D^*\bar{D}^*$ is the spin wave function. Our results show that in the molecular scenario, different spin-spin coupling may have a great impact on the strong decay properties. We take the $J/\psi\pi$ decay mode as an example. In Table IV, the spin factor for the coupling with $D\bar{D}^*$ is 3 times larger than that of $D^*\bar{D}^*$ in Figs. 1($C1$) and 1($T1$). The hyperfine interaction is expected to be more important for the $J/\psi\pi$ decay mode of $Z_c(3900)$. Moreover, our calculation shows that the hyperfine interaction for $Z_c(3900)$ plays a quite important role in Fig. 1 ($C1$) and even changes the sign of its amplitude.

As for $Z_c(4430)$, in the molecular scenario, we take it as an S-wave $D(2S)\bar{D}^*$ molecular state. Similarly we change the size of the molecular state in the range of $r_{\rm mean} = (1.0 \sim 3.0)$ fm, and we obtain

$$R^{\rm th}_{Z_c(4430)} \sim (1.4 \sim 1.3) \tag{37}$$

for $Z_c(4430)$ with a mass of $M = 4478$ MeV (see Fig. 3). Meanwhile, the partial widths of the $\eta_c\rho$ and $J/\psi\pi$ modes as the function of $r_{\rm mean}$ for $Z_c(4430)$ are shown in Fig. 4 as well. According to the figure, the decay properties of the $D(2S)\bar{D}^*$ molecular state are similar to the $D^*\bar{D}^*$ molecular state.

Fixing $r_{\rm mean} \simeq 1.00$ fm, we further obtain

$$\begin{aligned}\Gamma[Z_c(4430) \to \eta_c\rho] &\sim 1.28 \text{ MeV},\\ \Gamma[Z_c(4430) \to J/\psi\pi] &\sim 0.94 \text{ MeV}.\end{aligned} \tag{38}$$

At present, the charged state $Z_c(4430)$ was observed in both the $\psi'\pi^\pm$ and $J/\psi\pi^\pm$ channels [9–14], and it has not been reported in the $\eta_c\rho$ channel. According to our theoretical predictions, if $Z_c(4430)$ is a $D(2S)\bar{D}^*$ molecular state, the partial width of $\eta_c\rho$ is comparable to that of $J/\psi\pi$, which indicates that this state may be observed in the $\eta_c\rho$ channel as well.

Thus far, we have obtained the decay ratios in the molecular scenario. We find that the ratios are not sensitive to the relative molecular wave function in the loosely bound system, while the partial decay widths are very sensitive to the size of the molecules because of the sensitivity of the effective potentials.

B. The tetraquark scenario

In the tetraquark scenario, we obtain the decay ratio for the $Z_c(3900)$ state

$$R^{\rm th}_{Z_c(3900)} \sim 1.6, \tag{39}$$

which agrees with the experimental result (see Table X).

The predicted partial decay widths of the $\eta_c\rho$ and $J/\psi\pi$ modes are

$$\begin{aligned}\Gamma[Z_c(3900) \to \eta_c\rho] &\sim 0.23 \text{ MeV},\\ \Gamma[Z_c(3900) \to J/\psi\pi] &\sim 0.14 \text{ MeV}.\end{aligned} \tag{40}$$

Imitating the wave function of $Z_c(3900)$, we estimate the wave function of $Z_c(4020)$ as listed in Table VII. Similarly

TABLE X. The partial decay widths (MeV) for $Z_c(3900)$ and $Z_c(4020)$ as the tetraquark states. $R^{\rm th}$ and $R^{\rm exp}$ are the theoretical and experimental ratios, respectively.

State	$\Gamma[\eta_c\rho]$	$\Gamma[J/\psi\pi]$	$R^{\rm th}$	$R^{\rm exp}$
$Z_c(3900)$	0.23	0.14	1.6	2.2 ± 0.9
$Z_c(4020)$	0.19	0.12	1.6	...

we fix the mass of $Z_c(4020)$ at $M = 4024.1$ MeV and obtain

$$\Gamma[Z_c(4020) \to \eta_c\rho] \sim 0.19 \text{ MeV},$$
$$\Gamma[Z_c(4020) \to J/\psi\pi] \sim 0.12 \text{ MeV}. \quad (41)$$

Then the predicted partial decay width ratio is

$$R^{\rm th}_{Z_c(4020)} \sim 1.6. \quad (42)$$

The decay properties of $Z_c(4020)$ are similar in the molecular and tetraquark scenarios. Thus, besides the decay ratios, more precise experimental information is required to pin down the inner structure of this state.

As shown in Table X, the partial widths of the $\eta_c\rho$ and $J/\psi\pi$ decay modes for $Z_c(4020)$ are comparable to those for $Z_c(3900)$,

$$\frac{\Gamma[Z_c(3900) \to \eta_c\rho]}{\Gamma[Z_c(4020) \to \eta_c\rho]} = 1.2, \quad (43)$$

$$\frac{\Gamma[Z_c(3900) \to J/\psi\pi]}{\Gamma[Z_c(4020) \to J/\psi\pi]} = 1.2. \quad (44)$$

The ratios are very different from those in Eqs. (35) and (36). As mentioned earlier, in the molecular scenario, the hyperfine interaction plays a quite important role for $Z_c(3900)$ in Fig. 2($C1$) and even changes the sign of its amplitude. Thus, the total amplitudes for $Z_c(3900)$ are much larger than those for $Z_c(4020)$. However, in the tetraquark scenario, the Coulomb and linear interactions are dominant for both states $Z_c(3900)$ and $Z_c(4020)$. There exists good evidence for $Z_c(3900)$ in the $\eta_c\rho$ and $J/\psi\pi$ channels experimentally, and no evidence for $Z_c(4020)$. Our results support the belief that the two states are more likely to be the molecular states.

For $Z_c(4430)$, with the estimated wave function, we plot the partial decay width ratio between the $\eta_c\rho$ and $J/\psi\pi$ decay modes as a function of the effective size r_X of the tetraquark state (see Fig. 5). We find that the ratio depends slightly on r_X. Varying r_X in the range $r_X = (0.5\text{–}2.0)$ fm, the ratio is

$$R^{\rm th}_{Z_c(4430)} \sim (1.7 \sim 1.4), \quad (45)$$

which is slightly larger than that for a molecular state. According to our results, the branching fraction ratio between the $\eta_c\rho$ and $J/\psi\pi$ modes of $Z_c(4430)$ as a molecule or a tetraquark state is larger than 1, which indicates that $Z_c(4430)$ decays more easily into the $\eta_c\rho$ channel.

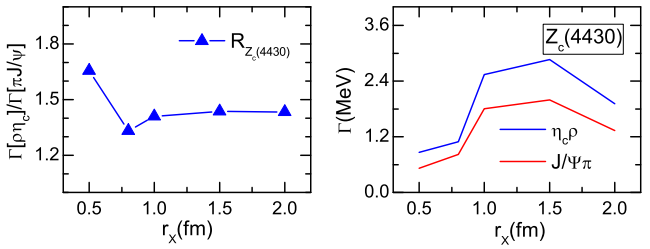

FIG. 5. (Left panel) The branching fraction ratio between the $\eta_c\rho$ and $J/\psi\pi$ channels for $Z_c(4430)$ in the tetraquark scenario. (Right panel) The partial decay widths for $Z_c(4430)$ decaying into the $\eta_c\rho$ and $J/\psi\pi$ channels in the tetraquark scenario.

Thus far, we have calculated the decay ratios of the $Z_c(3900)$, $Z_c(4020)$, and $Z_c(4430)$ decaying into the $\eta_c\rho$ and $J/\psi\pi$ channels in the molecular and tetraquark scenarios. Our results show that the decay ratios in both scenarios are similar. We cannot determine the inner structures only with the decay ratios. However, if we look at the partial decay widths, we find that in molecular scenario, $\Gamma(Z_c(3900) \to J/\psi\pi)$ are much larger than $\Gamma(Z_c(4020) \to J/\psi\pi)$, while they are similar in the tetraquark scenario. In experiments, the $Z_c(3900)$ state is observed in the $J/\psi\pi$ invariant mass spectrum while no significant $Z_c(4020)$ signal is observed. This may support the states $Z_c(3900)$ and $Z_c(4020)$ as the molecules instead of tightly bound tetraquark states.

IV. SUMMARY

In this work, we calculate the branching fraction ratios between the $\eta_c\rho$ and $J/\psi\pi$ decay modes for the charged states $Z_c(3900)$, $Z_c(4020)$, and $Z_c(4430)$ with a quark interchange model. In order to compare the decay properties in different physical scenarios and pin down the inner structure of these three mysterious charmoniumlike states, we study the ratios in the molecular and tetraquark scenarios, respectively. Meanwhile, we estimate the absolute partial decay widths for the $\eta_c\rho$ and $J/\psi\pi$ decay channels. Our main results are summarized as follows.

For $Z_c(4430)$, the branching fraction ratio as an S-wave $D(2S)\bar{D}^*$ molecule ($R^{\rm th}_{Z_c(4430)} \simeq 1.4$) is slightly smaller than that in the tetraquark scenario ($R^{\rm th}_{Z_c(4430)} \simeq 1.7 \sim 1.4$). We notice that the ratios in both physical scenarios are larger than 1, which indicates that $Z_c(4430)$ prefers to decay into the $\rho\eta_c$ channel rather than the $\pi J/\psi$ channel. Besides the $\pi J/\psi$ channel, $\rho\eta_c$ may be another interesting channel for the observation of $Z_c(4430)$ in future experiments.

For $Z_c(3900)$, we obtain the result that the ratios are $R^{\rm th}_{Z_c(3900)} \sim 1.3$ and 1.6 in the molecular and tetraquark

scenarios, respectively. Both are comparable to the experimental result. For $Z_c(4020)$, the ratios are $R^{\rm th}_{Z_c(4020)} \sim 2.4$ and 1.6, respectively. The above results show that the ratios in both scenarios are similar to each other. Thus, to investigate the inner structures, considering only the decay ratio R of the Z_c itself is not enough.

In the molecular scenario, the partial decay widths of the $\eta_c\rho$ and $J/\psi\pi$ modes for $Z_c(4020)(D^*\bar{D}^*)$ are smaller than those for $Z_c(3900)(D\bar{D}^*)$ by 1 order. In the molecular scenario, different spin-spin coupling may have a great impact on the strong decay properties. On the other side, the partial decay widths of the $\eta_c\rho$ and $J/\psi\pi$ modes for $Z_c(4020)(D^*\bar{D}^*)$ are comparable to those for $Z_c(3900)$ in the tetraquark scenario. At present, there exists good evidence for $Z_c(3900)$ in the $\eta_c\rho$ and $J/\psi\pi$ channels experimentally, and no evidence for $Z_c(4020)$. Our results indicate that these two states are more likely to be the moleculelike states which arise from the $D^{(*)}\bar{D}^{(*)}$ hadronic interactions.

ACKNOWLEDGMENTS

We would like to thank Xiao-Lin Chen and Wei-Zhen Deng for the very helpful suggestions. This work is supported by the National Natural Science Foundation of China under Grants No. 11947048 and No. 11975033. G.-J. W. is supported by China Postdoctoral Science Foundation Grant No. 2019M660279.

[1] S. K. Choi *et al.* (Belle Collaboration), Observation of a Narrow Charmoniumlike State in Exclusive $B^{+-} \to K^{+-}\pi^+\pi^- J/\psi$ Decays, Phys. Rev. Lett. **91**, 262001 (2003).
[2] M. Tanabashi *et al.* (Particle Data Group), Review of particle physics, Phys. Rev. D **98**, 030001 (2018).
[3] H. X. Chen, W. Chen, X. Liu, and S. L. Zhu, The hidden-charm pentaquark and tetraquark states, Phys. Rep. **639**, 1 (2016).
[4] Y. R. Liu, H. X. Chen, W. Chen, X. Liu, and S. L. Zhu, Pentaquark and Tetraquark states, Prog. Part. Nucl. Phys. **107**, 237 (2019).
[5] N. Brambilla, S. Eidelman, C. Hanhart, A. Nefediev, C. P. Shen, C. E. Thomas, A. Vairo, and C. Z. Yuan, The *XYZ* states: Experimental and theoretical status and perspectives, arXiv:1907.07583.
[6] F. K. Guo, C. Hanhart, U. G. Meiner, Q. Wang, Q. Zhao, and B. S. Zou, Hadronic molecules, Rev. Mod. Phys. **90**, 015004 (2018).
[7] A. Esposito, A. Pilloni, and A. D. Polosa, Multiquark resonances, Phys. Rep. **668**, 1 (2017).
[8] A. Hosaka, T. Iijima, K. Miyabayashi, Y. Sakai, and S. Yasui, Exotic hadrons with heavy flavors: X, Y, Z, and related states, Prog. Theor. Exp. Phys. **2016**, 062C01 (2016).
[9] S. K. Choi *et al.* (Belle Collaboration), Observation of a Resonancelike Structure in the $\pi^\pm\psi'$ Mass Distribution in Exclusive $B \to K\pi^\pm\psi'$ Decays, Phys. Rev. Lett. **100**, 142001 (2008).
[10] B. Aubert *et al.* (*BABAR* Collaboration), Search for the $Z(4430)^-$ at *BABAR*, Phys. Rev. D **79**, 112001 (2009).
[11] R. Mizuk *et al.* (Belle Collaboration), Dalitz analysis of $B \to K\pi^+\psi'$ decays and the $Z(4430)^+$, Phys. Rev. D **80**, 031104 (2009).
[12] K. Chilikin *et al.* (Belle Collaboration), Experimental constraints on the spin and parity of the $Z(4430)^+$, Phys. Rev. D **88**, 074026 (2013).
[13] K. Chilikin *et al.* (Belle Collaboration), Observation of a new charged charmoniumlike state in $\bar{B}^0 \to J/\psi K^-\pi^+$ decays, Phys. Rev. D **90**, 112009 (2014).
[14] R. Aaij *et al.* (LHCb Collaboration), Observation of the Resonant Character of the $Z(4430)^-$ State, Phys. Rev. Lett. **112**, 222002 (2014).
[15] L. Ma, X. H. Liu, X. Liu, and S. L. Zhu, Exotic four quark matter: $Z_1(4475)$, Phys. Rev. D **90**, 037502 (2014).
[16] L. Maiani, A. D. Polosa, and V. Riquer, The charged Z (4433): Towards a new spectroscopy, arXiv:0708.3997.
[17] D. Ebert, R. N. Faustov, and V. O. Galkin, Excited heavy tetraquarks with hidden charm, Eur. Phys. J. C **58**, 399 (2008).
[18] L. Maiani, F. Piccinini, A. D. Polosa, and V. Riquer, The $Z(4430)$ and a new paradigm for spin interactions in tetraquarks, Phys. Rev. D **89**, 114010 (2014).
[19] D. V. Bugg, How resonances can synchronise with thresholds, J. Phys. G **35**, 075005 (2008).
[20] S. X. Nakamura and K. Tsushima, $Z_c(4430)$ and $Z_c(4200)$ as triangle singularities, Phys. Rev. D **100**, 051502 (2019).
[21] M. Ablikim *et al.* (BESIII Collaboration), Observation of a Charged Charmoniumlike Structure in $e^+e^- \to \pi^+\pi^- J/\psi$ at $\sqrt{s} = 4.26$ GeV, Phys. Rev. Lett. **110**, 252001 (2013).
[22] Z. Q. Liu *et al.* (Belle Collaboration), Study of $e^+e^- \to \pi^+\pi^- J/\psi$ and Observation of a Charged Charmoniumlike State at Belle, Phys. Rev. Lett. **110**, 252002 (2013).
[23] T. Xiao, S. Dobbs, A. Tomaradze, and K. K. Seth, Observation of the charged hadron $Z_c^\pm(3900)$ and evidence for the neutral $Z_c^0(3900)$ in $e^+e^- \to \pi\pi J/\psi$ at $\sqrt{s} = 4170$ MeV, Phys. Lett. B **727**, 366 (2013).
[24] M. Ablikim *et al.* (BESIII Collaboration), Observation of a Charged Charmoniumlike Structure $Z_c(4020)$ and Search for the $Z_c(3900)$ in $e^+e^- \to \pi^+\pi^- h_c$, Phys. Rev. Lett. **111**, 242001 (2013).
[25] X. Liu, Z. G. Luo, Y. R. Liu, and S. L. Zhu, $X(3872)$ and other possible heavy molecular states, Eur. Phys. J. C **61**, 411 (2009).
[26] F. Aceti, M. Bayar, J. M. Dias, and E. Oset, Prediction of a $Z_c(4000)$ $D^*\bar{D}^*$ state and relationship to the claimed $Z_c(4025)$, Eur. Phys. J. A **50**, 103 (2014).

[27] J. R. Zhang, Improved QCD sum rule study of $Z_c(3900)$ as a $\bar{D}D^*$ molecular state, Phys. Rev. D **87**, 116004 (2013).
[28] D. Chakrabarti and C. Mondal, Transverse charge and magnetization densities in holographic QCD, Eur. Phys. J. C **74**, 2962 (2014).
[29] F. S. Navarra, M. Nielsen, and M. E. Bracco, $D^*D\pi$ form-factor revisited, Phys. Rev. D **65**, 037502 (2002).
[30] F. Aceti, M. Bayar, E. Oset, A. Martinez Torres, K. P. Khemchandani, J. M. Dias, F. S. Navarra, and M. Nielsen, Prediction of an $I = 1$ $D\bar{D}^*$ state and relationship to the claimed $Z_c(3900)$, $Z_c(3885)$, Phys. Rev. D **90**, 016003 (2014).
[31] M. Albaladejo, F. K. Guo, C. Hidalgo-Duque, and J. Nieves, $Z_c(3900)$: What has been really seen?, Phys. Lett. B **755**, 337 (2016).
[32] W. Chen and S. L. Zhu, The vector and axial-vector charmoniumlike states, Phys. Rev. D **83**, 034010 (2011).
[33] L. Zhao, W. Z. Deng, and S. L. Zhu, Hidden-charm tetraquarks and charged Z_c states, Phys. Rev. D **90**, 094031 (2014).
[34] M. B. Voloshin, $Z_c(3900)$—What is inside?, Phys. Rev. D **87**, 091501 (2013).
[35] S. Patel, M. Shah, and P. C. Vinodkumar, Mass spectra of four-quark states in the hidden charm sector, Eur. Phys. J. A **50**, 131 (2014).
[36] L. Maiani, V. Riquer, R. Faccini, F. Piccinini, A. Pilloni, and A. D. Polosa, A $J^{PG} = 1^{++}$ charged resonance in the $Y(4260) \to \pi^+\pi^- J/\psi$ decay?, Phys. Rev. D **87**, 111102 (2013).
[37] C. Deng, J. Ping, H. Huang, and F. Wang, Systematic study of Z_c^+ family from a multiquark color flux-tube model, Phys. Rev. D **92**, 034027 (2015).
[38] A. P. Szczepaniak, Triangle singularities and XYZ quarkonium peaks, Phys. Lett. B **747**, 410 (2015).
[39] D. Y. Chen and X. Liu, Predicted charged charmoniumlike structures in the hidden-charm dipion decay of higher charmonia, Phys. Rev. D **84**, 034032 (2011).
[40] D. Y. Chen, X. Liu, and T. Matsuki, Reproducing the $Z_c(3900)$ structure through the initial-single-pion-emission mechanism, Phys. Rev. D **88**, 036008 (2013).
[41] E. S. Swanson, Z_b and Z_c exotic states as coupled channel cusps, Phys. Rev. D **91**, 034009 (2015).
[42] E. S. Swanson, Cusps and exotic charmonia, Int. J. Mod. Phys. E **25**, 1642010 (2016).
[43] M. Ablikim *et al.* (BESIII Collaboration), Evidence for $Z_c^\pm$ decays into the $\rho^\pm\eta_c$ final state, Phys. Rev. D **100**, 111102 (2019).
[44] F. Goerke, T. Gutsche, M. A. Ivanov, J. G. Korner, V. E. Lyubovitskij, and P. Santorelli, Four-quark structure of $Z_c(3900)$, $Z(4430)$, and $X_b(5568)$ states, Phys. Rev. D **94**, 094017 (2016).
[45] S. Patel, M. Shah, K. Thakkar, and P. C. Vinodkumar, Decay widths of di-mesonic molecular states as candidates for Z_c and Z_b, Proc. Sci., Hadron2013 (**2013**) 189.
[46] A. Esposito, A. L. Guerrieri, and A. Pilloni, Probing the nature of $Z_c^{(\prime)}$ states via the $\eta_c\rho$ decay, Phys. Lett. B **746**, 194 (2015).
[47] H. W. Ke, Z. T. Wei, and X. Q. Li, Is $Z_c(3900)$ a molecular state, Eur. Phys. J. C **73**, 2561 (2013).
[48] J. M. Dias, F. S. Navarra, M. Nielsen, and C. M. Zanetti, $Z_c^+(3900)$ decay width in QCD sum rules, Phys. Rev. D **88**, 016004 (2013).
[49] Z. G. Wang and J. X. Zhang, The decay width of the $Z_c(3900)$ as an axial-vector tetraquark state in solid quark-hadron duality, Eur. Phys. J. C **78**, 14 (2018).
[50] S. S. Agaev, K. Azizi, and H. Sundu, Strong $Z_c^+(3900) \to J/\psi\pi^+$; $\eta_c\rho^+$ decays in QCD, Phys. Rev. D **93**, 074002 (2016).
[51] H. X. Chen, Decay properties of the $Z_c(3900)$ through the Fierz rearrangement, arXiv:1910.03269.
[52] T. Barnes, N. Black, and E. S. Swanson, Meson meson scattering in the quark model: Spin dependence and exotic channels, Phys. Rev. C **63**, 025204 (2001).
[53] T. Barnes, N. Black, D. J. Dean, and E. S. Swanson, BB intermeson potentials in the quark model, Phys. Rev. C **60**, 045202 (1999).
[54] J. P. Hilbert, N. Black, T. Barnes, and E. S. Swanson, Charmonium-nucleon dissociation cross sections in the quark model, Phys. Rev. C **75**, 064907 (2007).
[55] E. S. Swanson, Intermeson potentials from the constituent quark model, Ann. Phys. (N.Y.) **220**, 73 (1992).
[56] T. Barnes and E. S. Swanson, A diagrammatic approach to meson meson scattering in the nonrelativistic quark potential model, Phys. Rev. D **46**, 131 (1992).
[57] C. Y. Wong, E. S. Swanson, and T. Barnes, Heavy quarkonium dissociation cross-sections in relativistic heavy ion collisions, Phys. Rev. C **65**, 014903 (2001).
[58] S. Godfrey and N. Isgur, Mesons in a relativized quark model with chromodynamics, Phys. Rev. D **32**, 189 (1985).
[59] S. Weinberg, Elementary particle theory of composite particles, Phys. Rev. **130**, 776 (1963).
[60] S. Weinberg, Quasiparticles and the born series, Phys. Rev. **131**, 440 (1963).